Fast ignitor research at the Institute of Laser Engineering, Osaka University*

R. Kodama,† K. Mima, K. A. Tanaka, Y. Kitagawa, H. Fujita, K. Takahashi, A. Sunahara, K. Fujita, H. Habara, T. Jitsuno, Y. Sentoku, T. Matsushita, T. Miyakoshi, N. Miyanaga, T. Norimatsu, H. Setoguchi, T. Sonomoto, M. Tanpo, Y. Toyama, and T. Yamanaka
Institute of Laser Engineering, Osaka University, 2-6 Yamada-oka, Suita, Osaka 565-0871, Japan

(Received 24 October 2000; accepted 10 January 2001)

The physics element relevant to the fast ignitor in inertial confinement fusion has been extensively studied. Laser-hole boring with enormous photon pressures into overcritical densities was experimentally proved by density measurements with XUV laser probing. Ultra-intense laser interactions at a relativistic parameter regime were studied with a 50-TW glass laser system and a 100-TW glass laser system synchronized with a long pulse laser system. In the study of relativistic laser beam propagation in a 100-μm scale-length plasma, a special propagation mode (super-penetration mode) was observed, where the beam propagated into overdense regions close to the solid target surface. At the super-penetration mode, 20% of the laser energy converted to energetic electrons toward the target inside, while the coupling efficiency was 40% without the long scale-length plasmas. The high-density energetic electron transport and heating of solid material was also studied, indicating beamlike propagation of the energetic electrons in the solid target and effective heating of solid density ions with the electrons. Based on these basic experimental results, the heating of imploded plasma by short-pulse-laser light with three different ways of injecting the heating pulse has been studied. © *2001 American Institute of Physics.* [DOI: 10.1063/1.1352598]

I. INTRODUCTION

In the course of our experiments, high-density compression was realized at more than 600 times of liquid density with laser implosion.[1] The high-density of the imploded plasmas was close to that required for laser fusion ignition, but the temperature of the compressed core plasma was less than our expectation because of the mixing of core plasmas due to fluid instabilities.[1] One of the approaches to this problem is control or reduction of the fluid instabilities to recover the missing kinetic energy or to create the central hot spark structure in the compressed core plasmas. Another approach is externally enforced heating of the core plasmas. A fast ignitor (FI) concept was proposed as the second approach to efficiently ignite the high-density fusion fuel plasmas with ultra-intense short-pulse-laser light.[2] This concept is to inject ultra-intense laser light into the high-density imploded core plasmas within the core disassembling time (less than a few 10 ps). During the last several years, the progress of ultra-intense lasers such as 100 TW-PW lasers[3] has enabled us to study the physics elements of the FI concept, such as relativistic laser plasma interactions.

In the FI concept, one of the critical issues is efficient propagation of laser light into high-density regions in long scale-length plasmas surrounding the imploded core plasma. Laser-hole boring[4] with enormous photon pressures could be one of the candidates to efficiently guide the heating pulse to the high-density regions. Relativistic transparency[5] with relativistic self-focusing[6] might also be expected to induce self-guiding of the relativistic laser light into high-density regions. The other critical issues among the physics elements in the FI concept are generation of energetic particles and transport. The generation efficiency of the high-energy particles to the target inside is especially important in long scale-length plasmas. Transport of high-density relativistic electrons above the Alfvén limit must also be a most important issue to be studied for the heating of high-density plasmas. Based on understanding of the physics elements in the FI concept, we can start the investigation of enforced heating of imploded plasmas with ultra-intense laser light.

In this paper, we summarize (Sec. III) the extensive studies of the physics elements, such as laser-hole boring, relativistic laser propagation in long scale-length plasmas, generation of energetic particles, energy transport of high-density energetic electrons, and heating of ions with the electrons. Taking account of these experimental results on the physics elements, approaches to imploded plasma heating with short pulse lasers with three different methods for short pulse laser injection into the imploded plasmas are presented in Sec. IV.

II. LASER CONDITION FOR THE EXPERIMENTS

All the experimental results presented here were obtained by using the 50-TW short-pulse-laser system (GEKKO MII)[7] and 100-TW short pulse laser system[8] coupled with the GEKKO XII laser system at the Institute of Laser Engineering (ILE), Osaka Univ. Both laser systems provided a 1.05-μm chirped pulse giving 0.7–1 ps for the

*Paper HI3 3, Bull. Am. Phys. Soc. **45**, 160 (2000).
†Invited speaker.

100-TW laser system and 0.5 ps for the 50-TW system. The short-pulse-laser light was focused with an $f/3.6$ on-axis parabola for the 100-TW system and with an $f/3.3$ off-axis parabola for the 50-TW systems. The spot size for both systems was 20–30 μm in vacuum at the best focus position from x-ray pinhole images, giving peak on-target intensities of $(0.5-1)\times10^{19}\,\mathrm{W/cm^2}$. Long scale-length preformed plasmas were created with 100-ps or 1-ns Gaussian laser pulses from the GEKKO XII systems, which were synchronized with the 100-TW system within a time jitter of less than 100 ps. The preformed plasmas in the basic experiments were created by 0.53-μm laser light from the three beams of the long-pulse-laser system. The intensities on the target were $10^{14}\,\mathrm{W/cm^2}$ to $10^{15}\,\mathrm{W/cm^2}$ with a spot diameter of 500 μm. The scale-length of the preformed plasma was estimated from a hydrodynamic simulation checked experimentally with UV and XUV probing.[9–11] The critical density (n_c) point was located at about 100 μm from the target surface and the scale-length was about 200 μm from the n_c point to the under-dense region. Implosion plasmas or spherical geometry plasmas were created by a 1-ns Gaussian pulse or a 1.5-ns square pulse from the GEKKO XII systems. A 0.53-μm laser light from 9 to 12 beams of the long pulse laser system was focused with aspherical lenses of $f/3$ through random phase plates to uniformly illuminate the spherical target at an intensity of about $10^{14}\,\mathrm{W/cm^2}$.

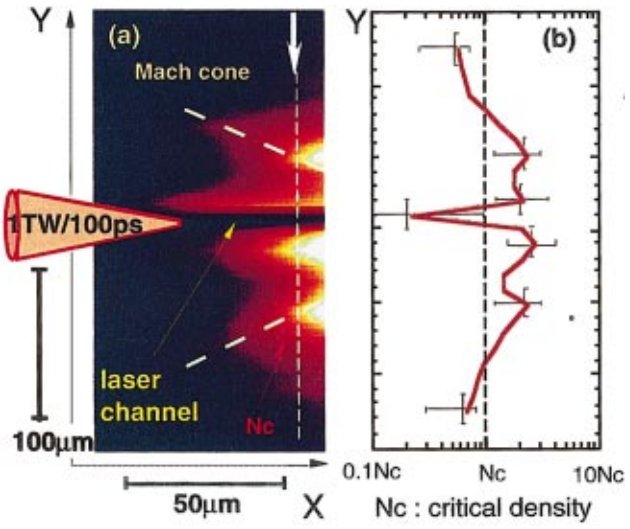

FIG. 1. (Color) (a) Electron density contour from the XUV laser refractometry, indicating laser-hole boring into overdense regions and the Mach cone due to the supersonic propagation of the channel front. (b) Transverse electron density profile at 55 μm from the target surface, showing a density well on the laser axis with a width of less than 30 μm.

III. ELEMENTARY PHYSICS IN THE FAST IGNITOR

We have extensively studied intense-laser plasma interactions as elementary physics of the FI. Investigated were laser-hole boring into overdense regions, propagation of relativistic laser beam in long scale inhomogeneous plasmas, energetic electron generation and its transport. All the experiments were carried out using plane targets.

A. Laser-hole boring

Laser-hole boring experiments were performed by using a 100-ps laser pulse with a wavelength of 1.053 μm. A 100-μm scale-length plasma was created on a plastic (CH) plane target with a thickness of 100 μm. The 1.053-μm laser light was normally focused onto the preformed plasma at a peak intensity of $2\times10^{17}\,\mathrm{W/cm^2}$ in vacuum. Details of the experimental conditions are presented in Refs. 4 and 9. The laser channel formation in the preformed plasma was measured by using four kinds of diagnostics. Electron density profiles at under-critical densities ($10^{19-20}\,\mathrm{cm^{-3}}$) were measured by using a UV (263-nm) interferometer system with a temporal resolution of 10 ps.[10] Properties of the laser turning point close to the critical density were monitored by measurements of a Doppler shift of the backscattered light spectra and the second-harmonic-light spectra. The channel formation into the overdense region ($-10^{22}\,\mathrm{cm^{-3}}$) was directly measured with an XUV laser (19.6-nm) probe system.[11] Laser energy deposition at densities close to the solid density was monitored with an x-ray pinhole camera (1 to 30 keV).

Figure 1(a) shows a typical electron density contour from XUV laser probing and Fig. 1(b) shows an electron density profile in the transverse direction to the axis of the channeling beam. The channel beam was focused on the preformed plasma at 210–250 μm distance from the target surface. A clear density well is seen on the laser axis into overdense regions, indicating laser-hole boring with photon pressures. The channel width was less than 30 μm at 50–60 μm distance from the target surface, corresponding to 150–200 μm from the focus position. A width of the laser profile less than 26 μm could be required to explain the density profile from a simple estimation given by an equilibrium condition between the ponderomotive force and thermal pressure for 1–10 keV. This result (laser propagation over 150–200 μm with <30 μm diameter for $f/3$) indicates laser self-focusing and channeling into overdense plasmas. Another ridge of the density humps, diverging along the channel in the direction opposite to the laser beam, appeared at outer regions from the channel walls. Extrapolated lines of this ridge of the density hump cross at the target surface on the beam axis corresponding to the channel axis. These density humps may indicate a Mach cone of the shock waves created by supersonic propagation of the channel front. From a Doppler shift of the back scattered light spectra showing a front speed of 7×10^7 cm/s, the angle of the Mach cone is estimated to be 43 deg for a plasma temperature of 3 keV. This Mach cone angle from the front speed is consistent with the experimental observation (45 deg).[9]

All of the data presented above are consistent with each other, indicating whole beam self-focusing of the laser light into the overdense region at an appropriate focus condition. The focus position of the laser light will affect the ponderomotive self-focusing in the underdense region, which may change the intensity of the laser light in the channel and the spatial profile of the beam at the critical density. This effect in the underdense region might increase the distance of laser propagation into overdense regions.

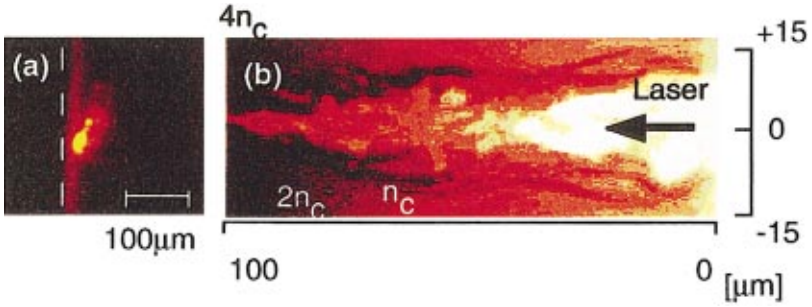

FIG. 2. (Color) (a) X-ray pinhole image (1–30 keV) from target tangential at a focusing position of 200 μm from the target surface and (b) ion density map at 1.1 ps after the start of the laser pulse from the 2D PIC simulation, indicating whole beam self-focusing into overdense regions close to the target surface.

B. Relativistic beam penetration

Laser propagation experiments were conducted changing the focal position of the 100-TW beam along the laser axis relative to the preformed plasma. The focal position was varied from 50 μm to 1.5 mm from the original target surface. X-ray hot spots as shown in Fig. 2(a) appeared on the target surface when the laser focus positions, d, were set at almost $d=150\,\mu$m to $d=230\,\mu$m from the surface, corresponding to $0.5n_c-0.8n_c$ from hydrodynamic simulation results checked with other experiments.[11] No such strong hot spots were obtained at $d=50\,\mu$m–1.5 mm except for the window of $d=150\,\mu$m–$d=230\,\mu$m. This typical image shows the localization of x-ray emission along the laser axis at near solid densities and partially separated from the target surface, indicating energy deposition of laser light with a short absorption length. When the hot spot appeared on the target surface, we always observed jetlike x-ray emission induced by specularly reflected light from the high-density region, as shown in Ref. 12. The jet formation will also support the laser light penetration into the high-density region close to the target surface.[12,13] The short-pulse-laser light could be self-focused in the long scale-length plasmas.[14] The self-focused beam would penetrate into the high-density region following the relativistic electrons propagation, as mentioned in Ref. 15. This self-focused channel close to the target surface is named super-penetration.[16] The experimental results of x-ray images, x-ray laser probing, and back-scattered spectra on laser-hole boring into overdense plasmas[4,9] also support that the ultra-intense laser light has penetrated in this long scale preformed plasmas up to regions close to the solid target surface. Figure 2(b) shows the ion density map at 1.1 ps from two-dimensional (2D) particle-in-cell (PIC) simulations, showing whole beam self-focusing into $2n_c$ close to the target surface at this density profile. The PIC simulation shows that filamentation is induced by hot electrons and magnetic fields created in the underdense plasmas at the beginning. Later several filaments are combined to be one single hole as shown in Fig. 2(b). Although more detailed discussions should follow to explain the difference and the mechanism of these propagation modes, clearly seen in both cases is that the laser beam can relativistically self-focus in the plasma and can propagate through low-density channels into the overdense plasmas. These results are fully consistent with the x-ray images indicating super-penetration of laser light into high-density regions.

C. Generation of energetic electrons

Generation of energetic particles was measured both inside and outside the target. The energetic electron spectra were obtained with an electron spectrometer from 30 deg to the laser axis, as shown in Fig. 3. The temperature of the energetic electrons without the long scale-length plasmas was 1.8 MeV to 2.2 MeV and 2.5 MeV to 3.8 MeV in the super-penetration mode with the long scale-length plasmas. The spectra obtained with an electron spectrometer were well consistent with the 2D PIC simulations. The interaction with the long scale-length plasma creates higher-energy electrons. Beam self-focusing in the plasma can create higher-energy electrons due to the increase in the local intensity of the laser light. The simulation also indicates that magnetic fields in the channel in underdense plasmas (acceleration of electrons at betatron resonance[17]) could generate higher-energy electrons with >10 MeV in the laser direction. Generation of the energetic electrons with energies of less than a few MeV toward the target inside was also evaluated by absolute measurements of $K\alpha$ x-ray yield from the target back side layer. The target used in the experiments consisted of CD, Mo, and Ag layers with thicknesses of 30 μm, 50–300 μm, and 50 μm, respectively. The CD layer was irradiated with 0.53-μm laser light to create the long scale-length plasmas and the Ag layer was used as a $K\alpha$ emitter. To interpret the coupling efficiency of the energetic electrons to the target inside from the $K\alpha$ emission (Ag), we used a 3D Monte Carlo Electron

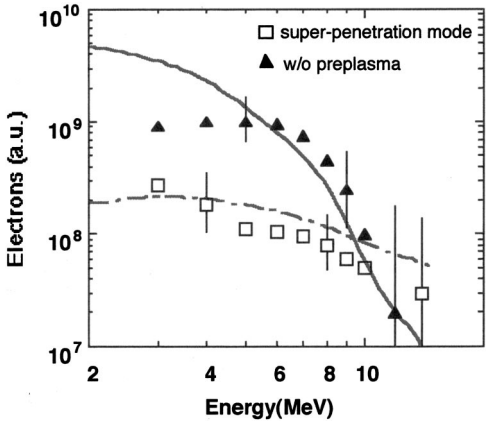

FIG. 3. Electron spectra obtained with the electron spectrometer and 2D PIC simulations for the shot without long scale-length plasmas and for the super-penetration with the long scale preformed plasmas.

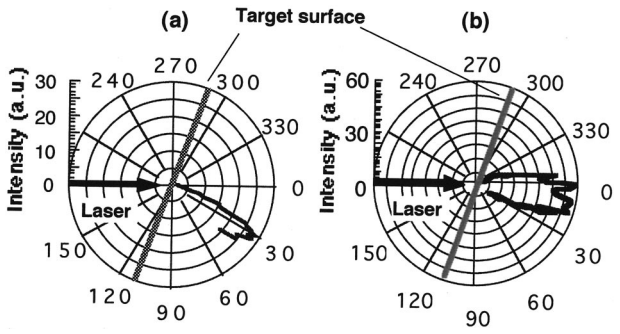

FIG. 4. Hard x-ray (0.3–1 MeV) angular distributions obtained with 50 pieces of TLDs at different scale-length of the preformed plasmas; (a) less than a few times λ and (b) more than 10 times λ.

Transport code. From the experimental results, the coupling efficiency from the laser to the energetic electrons toward the target interior is estimated to be less than a few percent for the interactions with the long scale-length plasmas. However, the coupling efficiency of 20%–25% was obtained only for the super-penetration mode in the interactions with the long scale-length plasmas (cf. The coupling efficiency without the long scale-length plasma was about 40%). PIC simulation shows that most of the laser light is absorbed at the channel wall in the long scale plasma before reaching the high-density regions and generates electrons in the vertical directions. However, in the super-penetration mode, the laser light could reach the high-density region and create a steep density gradient with the photon pressure, causing the absorption via **J×B** heating at the steep density boundary.[18] The photon pressure of Gaussian profile laser light also changes the channel front figure to concave, resulting in the oblique incidence interaction of the light locally at the channel front to generate electrons into the target interior from the simulation. In the PIC simulation for the case without the preformed plasmas, 70% of the absorbed laser energy or electron energy contributes to the electrons accelerated in the laser direction to create the $K\alpha$ emission. On the other hand, only 15% of the absorbed laser energy is coupled to the electrons in the laser direction even for the super-penetration mode in the preformed plasma. Most of the laser energy is absorbed at the channel wall by electrons in the vertical directions in the long scale-length plasmas, which is energy loss from the viewpoint of energy coupling to the electrons in the laser direction. Therefore, higher coupling such as 40% to the electrons in the laser direction could be realized for the interaction without long-scale preformed plasmas.

The direction of the energetic electrons at different scale-lengths of the preformed plasma was studied by measurements of hard x-ray angular distribution with a TLD array consisted of 50 pieces of the detectors as shown in Fig. 4. Both of the angular distributions indicate collimating of electron propagation in the target. At the small scale-length, the direction of the collimated x-rays is along the rear target normal and the direction for the longer scale-length corresponds to the laser direction. This difference in the direction of collimation could be explained by Brunel-type resonance absorption[19] being the dominant absorption in a plasma with a steep density gradient. As the scale-length increases, the **J×B** mechanism becomes the main production of the energetic electrons. In the long scale-length plasmas, the strong photon pressure of Gaussian profile laser light could create a steep density gradient at the front by itself and change the front figure to concave. This front deformation with the photon pressure might cause locally oblique-incidence interaction of the light and the Brunel-type absorption at the laser-channel front in the long scale-length plasma, which would also generate the electrons in the channel direction or laser directions.

D. Energy transport

Energy transport of energetic electrons was investigated by the study of heating properties of solid targets. Al solid targets were irradiated with 20-TW to 40-TW laser light at a *P*-polarization. The heating property of the target rear side was measured with a two-dimensional spatially-resolved UV high-speed sampling camera. The energetic electron heating was temporally separated from heating by a shock wave and/or a heat wave from the laser irradiation area. As the target thickness increases from 10 μm to 1 mm, the peak intensity of the heating area decreases with the increase in the heating area. The experimental result at 20-TW irradiation shows that the electron beam propagates as a single narrow beam for more than 200 μm and then breaks up into filaments at more than 500 μm. The divergence angle of the beam (full width half maximum, FWHM) before the break-up was about 20–30 deg. The filament structures, which appeared in the 20-TW laser interaction with the thicker target, changed to collapsed at 40-TW irradiation. At higher laser power, one could expect energetic electrons with a higher current in the target, resulting in a higher magnetic field that pinches the filament. This electron propagation was also observed in the interaction with long scale-length plasmas for the super-penetration mode. Figure 5(b) shows the rear side emission in the super-penetration mode (100-TW laser interaction), as well as the x-ray image [Fig. 5(a)] on the front side. The heating structure follows well the front x-ray structure, indicating beamlike propagation of the energetic electrons in the super-penetration mode. No significant localized heating region on the rear side and x-ray spot on the front side was obtained in the interactions with the long scale-length plasmas except for the super-penetration mode. Such localized heating was observed only for the super-penetration in the interaction with the long scale plasmas. This result is consistent with the high conversion efficiency to the energetic electrons to the target inside, such as 20%–25% at the super-penetration mode. High-density energetic electrons could generate a magnetic field, resulting in beamlike propagation in the target.

Ion temperatures of plasmas heated by these energetic electrons were also evaluated from measurements of thermal neutrons from CD_2 layered target. The laser irradiation side and the backside were coated with 10-μm Al foils and irradiated with 40-TW laser light. We observed clear neutron signals of the D-D thermal nuclear fusion reaction at 2.45 MeV on the time of flight (TOF) signals from two different

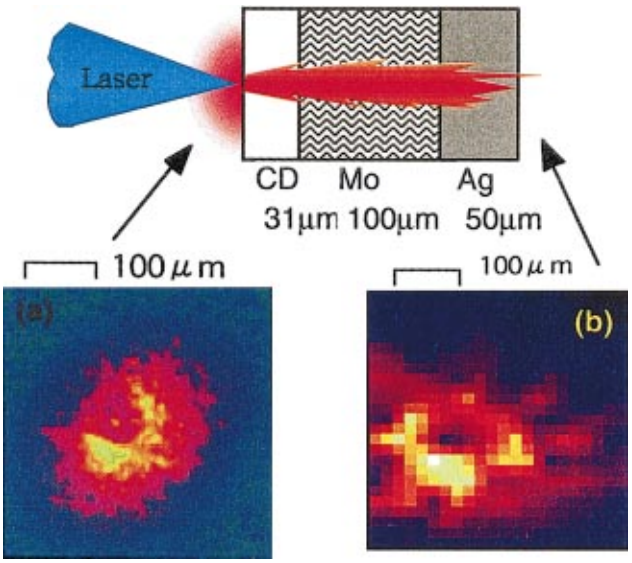

FIG. 5. (Color) (a) X-ray image (1–30 keV) of laser irradiation from the target front side at the super-penetration mode with the long scale-length plasmas and (b) UV framing image of the target rear side showing the area of energetic electron heating at the same shot.

observation angles. The yield of the neutrons was about $(1-4)\times 10^4$, indicating the ion temperature of about 500 eV, assuming that the heated volume was a cylinder with a spot diameter. This value implies effective heating of solid-density ions with the 40-TW laser light while more heating with higher power laser might require higher ion densities because of the thermal equilibration time from energetic electrons to ions.

III. HEATING OF IMPLOSION PLASMAS

Based on the investigation of the elementary physics, we are studying imploded plasma heating with three different ways as shown in Fig. 6. The critical issues for the investigations are how to inject the heating pulse into the high-density regions as close to the core plasma as possible. Long scale plasmas surrounding the core plasma prevent the ultra-intense laser light from effective propagation into the high-density regions. Laser-hole guiding, self-guiding of the relativistic heating pulse, and external solid-cone guiding are

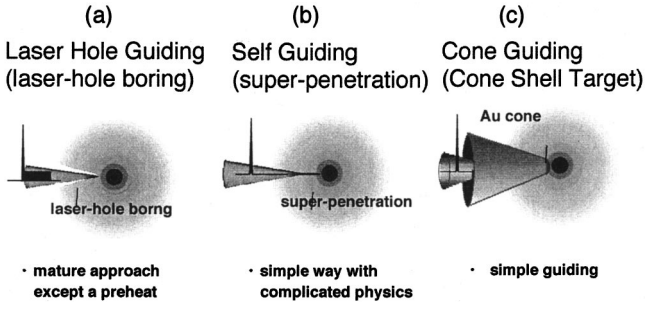

FIG. 6. Schema of three different methods to inject a heating pulse into high-density regions as close to the compressed core plasmas as possible. (a) Laser-hole guiding with precursorpulse boring into the high density; (b) self-guiding of the heating pulse with super-penetration; (c) external solid-cone guiding.

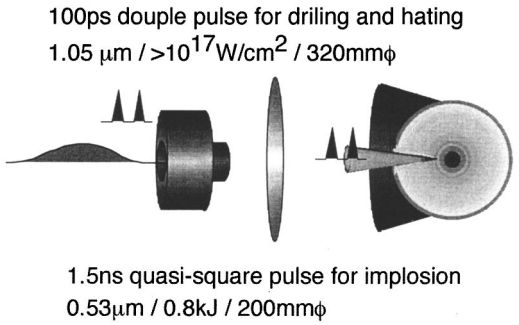

FIG. 7. Co-axial laser beam configuration consisting of 1.5 ns/0.53 μm axial beams for implosion and 100 ps/1 μm outer-ring beams for channeling on the GEKKO XII laser system to study the laser-hole guiding approach.

being studied for imploded plasma heating with short-pulse-laser light, taking into account the experimental results on the element physics.

A. Laser-hole guiding approach

One approach, as shown in Fig. 6(a), is to bore a laser-created channel into the overdense region with enormous photon pressures (laser-hole boring). The channel in the overdense regions will guide the heating pulse into the high-density regions. This approach would be mature except for the possibility of preheating of the shell before the maximum compression by hot electrons created by the channeling beam. In this approach, two successive 1.053 μm/100 ps pulses from one or two beams of the GEKKO XII were injected using the same focusing lens into the implosion plasma; the implosion plasmas were created with 12 beams of the GEKKO XII with a wavelength of 0.53 μm. These two kinds of beams were provided from two independent and synchronized-operated oscillators: one generated 1.5-ns quasi-square pulse for implosion and another for 100-ps pulses. These pulses were set up as co-axial beams consisting of a 1.5 ns/0.53 μm axial beam for implosion and a 100 ps/1.053 μm outer ring beam for laser-hole boring and/or heating on the GEKKO XII system, as shown in Fig. 7. CD shell targets with a diameter of 500 μm and a thickness of 5 μm were uniformly irradiated with the 12 axial beams to create imploded plasmas. The implosion plasma was irradiated with the 100-ps pulse from the two outer ring beams at an intensity of 10^{17} W/cm^2 in vacuum. From the basic experiments using plane targets, such double pulses with self-focusing could create hot electrons (100–200 keV) with a conversion efficiency of about 5%, which might effectively heat the compressed core plasma or preheat the shell before the maximum compression. When the double-short-pulse-laser light was injected at 100 μm off from the initial target surface, neutron yield, and x-ray emission increased as compared with those with neither injection of the beam nor different focus conditions. This implies that the injection beam, which depended on the focusing conditions, could self-focus into the implosion plasma. Mechanisms of the increase in the neutron yield are, however, not clear-whether shock heating, energetic heating, beam fusion due to accelerated ions or

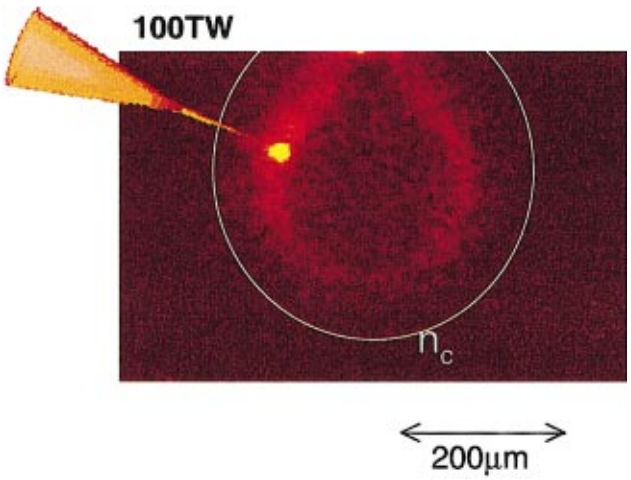

FIG. 8. (Color) X-ray pinhole camera image (1–30 keV), indicating super-penetration of 100-TW laser light in the spherical plasma. The long scale plasma was created on the 200-μm solid spherical CH target.

reduction in the shell density due to preheat by the channeling beam. Further study is required by changing the timing and focusing of the short pulse laser.

B. Super-penetration approach

The second approach, as shown in Fig. 6(b), is self-guiding of the heating pulse due to a relativistic nonlinear processes. Using the super-penetration mode, ultra-intense laser light can propagate directly into high-density regions close to the compressed core plasmas by itself. The propagated laser light will efficiently convert to energetic electrons in the laser direction with an efficiency of about 20% at the super-penetration mode. This approach is simple, but requires control of complex nonlinear processes such as relativistic self-focusing. To study the propagation mode in a spherical geometry, 100-μm scale-length plasmas were created on a solid sphere CH target with 12 beams of the GEKKO XII laser light. Laser light measuring 100-TW was focused on the long scale inhomogeneous plasmas changing the focusing positions. Only when focusing the beam at the location with 0.5–0.8 times the critical density was a strong x-ray hot spot observed on the spherical target surface, as shown in Fig. 8. This strong hot spot is similar to that observed in the basic experiments on the relativistic beam propagation using a plane target, indicating the super-penetration mode in the spherical geometry. This super-penetration mode has been applied to imploded plasmas with a CD shell target. CD shell targets of 500 μm with thicknesses of 6–7 mm were uniformly irradiated by 0.53-μm laser light with a laser energy of 2 kJ and the 100-TW laser light with energies of 50 J to 80 J was injected into the core plasmas. The implosion laser energy was limited in order to keep the initial internal energy of the imploded core plasma lower than the heating pulse energy. Changing the focus point of the heating pulse, an increase in the neutron yield was obtained only for the super-penetration mode. The neutron yield for the super-penetration mode was a few times 10^5, whereas the yield was about a few times 10^4 for no injection of the heating pulse. The yield of 10^5 was also not obtained at different focus points of the heating pulse from the super-penetration mode, i.e., 10^4. The observed neutrons could be mainly due to beam fusion reactions of accelerated ions by the heating pulse from neutron energy spectra (wing-like spectra appeared by both sides of 2.45 MeV), indicating the beam propagation into the high-density regions for the super-penetration mode. Evidence of imploded plasma heating from thermal neutrons above the beam fusion neutrons is expected on the neutron spectra when injecting 1-PW laser light into higher-density compressed core plasmas.

C. Cone guiding approach

As the third approach, an external solid cone is attached to the shell target to guide the heating short pulse laser to high-density regions, as shown in Fig. 6(c). The cone inside remains a vacuum and avoids beam propagation in the long scale-length plasmas. This approach has the advantage of effective propagation of the heating pulse into the high-density regions and a high conversion efficiency from the heating pulse energy to energetic electrons as high as 40%. One of the critical issues of this approach is implosion performance of the cone-shell target. To study this performance, we use a simple 2D hydrodynamic simulation code, where the initial condition is introduced from 1D hydrodynamic simulation. Figure 9 shows the density contours of imploded plasmas with the Au cone-shell target. An Au cone with an opening angle of 30 deg is set 50 μm from the center of the CD shell with an initial diameter of 500 μm and a thickness of 7 μm. The top of the cone is covered with a 2-μm Au foil. The shell is irradiated uniformly by 0.53-μm laser light with an energy of 4 kJ. The cone top sustains the maximum-

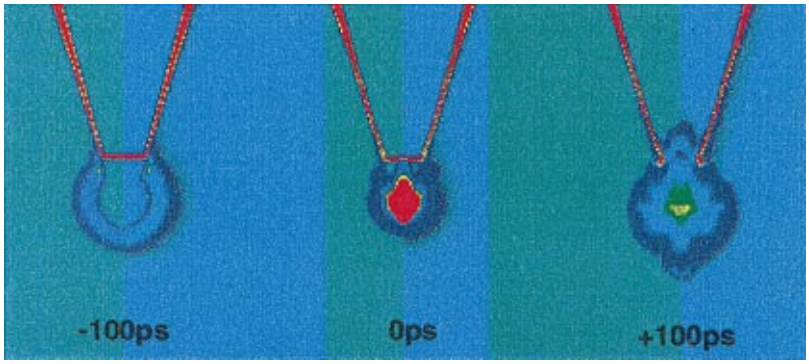

FIG. 9. (Color) Density contours of the cone-shell implosion at different times from 2D hydrodynamic simulation. *O* is corresponding to the maximum compression.

density compressed core plasma for a time and breaks out by the pressure of the core plasmas. The simulation indicates no significant difference in the density between a simple shell implosion and a cone-shell target implosion. The reduction of the density was only 20%–30% by attaching the cone. The temperature reduction will be more significant in the cone-shell implosion, which must be heated by the injection of the short-pulse-laser light at the maximum compression. We have experimentally demonstrated the implosion of the cone-shell target and the imploded plasma heating with 100-TW short-pulse-laser light.

IV. SUMMARY

We have investigated physics elements in the fast ignitor concept, such as laser-hole boring, relativistic beam propagation in long scale-length plasmas, generation of high-energy particles, and energy transport of high-density relativistic electrons. The laser-hole boring into overdense regions was realized and observed directly by XUV laser probing. Ponderomotive self-focusing could increase the penetration into higher-density regions at intensity of $2\times10^{17}\,\mathrm{W/cm^2}$. Short-pulse-laser light of 100 TW penetrated into the overdense regions close to the sold density with relativistic self-focusing and/or relativistic transparence (super-penetration) only when the laser was focused at 0.5–0.8 times of the critical density in the long scale-length plasmas. The energy conversion efficiency from the short pulse to energetic electrons into target inside was 40% without any long scale-length plasmas and 20%–25% with the long scale-length plasmas at the super-penetration mode at an intensity of $10^{19}\,\mathrm{W/cm^2}$. The high-density energetic electrons effectively propagated with divergence angles of less than 20–30 deg and heated Al solid targets with areal densities up to $0.3\ \mathrm{g/cm^2}$. Effective heating of ions in solid targets by energetic electrons was also proved by measurements of thermal neutrons from CD_2 targets. Taking account of these experimental results, three different methods on the short-pulse-laser injection to the imploded plasmas have been investigated to study enforced heating of imploded plasmas. One is laser drilled-hole guiding, the others are self guiding with the super-penetration mode and external solid cone guiding of the heating pulse to the core plasmas.

ACKNOWLEDGMENTS

We acknowledge all the technical support of the engineering staffs at ILE Osaka University for the laser operation, target fabrication and data acquisition. We especially thank Dr. H. Yoshida, K. Sawai, O. Maegawa, T. Kawaski, S. Matsuo, and K. Suzuki for their invaluable support.

[1] H. Azechi *et al.*, Laser Part. Beams **9**, 193 (1991).
[2] M. Tabak *et al.*, Phys. Plasmas **1**, 1626 (1994).
[3] M. D. Perry and G. Mourou, Science **264**, 917 (1994).
[4] R. Kodama *et al.*, Phys. Rev. Lett. **77**, 4906 (1996); R. Kodama *et al.*, Plasma Phys. Controlled Fusion **41**, A419 (1999).
[5] A. I. Akhiezer and R. V. Polovin, Sov. Phys. JETP **30**, 915 (1956); P. K. Kaw and J. Dawson, Phys. Fluids **13**, 472 (1970); J. Fuchs *et al.*, Phys. Rev. Lett. **80**, 1658 (1998).
[6] A. B. Borisov *et al.*, Phys. Rev. Lett. **65**, 1753 (1990); A. B. Borisov *et al.*, *ibid.* **68**, 2309 (1992).
[7] Y. Kitagawa *et al.*, Fusion Eng. Des. **44**, 261 (1999).
[8] Y. Kato *et al.*, Plasma Phys. Controlled Fusion **39**, A145 (1997).
[9] K. Takahashi *et al.*, Phys. Rev. Lett. **84**, 2405 (2000).
[10] K. A. Tanaka *et al.*, Phys. Rev. E **60**, 3283 (1999).
[11] R. Kodama *et al.*, Rev. Sci. Instrum. **70**, 543 (1999).
[12] R. Kodama *et al.*, Phys. Rev. Lett. **84**, 674 (2000).
[13] Y. Sentoku *et al.*, Phys. Plasmas **6**, 2855 (1999); H. Ruhl *et al.*, Phys. Rev. Lett. **82**, 743 (1999).
[14] M. Tatarakis *et al.*, Phys. Rev. Lett. **81**, 999 (1998); M. Borghesi *et al.*, *ibid.* **83**, 4309 (1999); L. Gremillet *et al.*, *ibid.* **83**, 5015 (1999).
[15] A. Pukhov *et al.*, Phys. Rev. Lett. **79**, 2686 (1997).
[16] K. A. Tanaka *et al.*, Phys. Plasmas **7**, 2014 (2000).
[17] A. Pukhov *et al.*, Phys. Plasmas **6**, 2847 (1999).
[18] W. E. Kruer and K Estabrook, Phys. Fluids **28**, 430 (1985).
[19] F. Brunel, Phys. Rev. Lett. **59**, 52 (1987).